Polymer Vol. 39 No. 16, pp. 3759–3766, 1998

0032-3861/98/$19.00+0.00

PII: S0032-3861(97)10145-8

Isothermal crystallisation of end-linked poly(tetrahydrofuran) networks. 3. Small-angle neutron scattering

Mitsuhiro Shibayama[a,*], Hiroshi Takahashi[a], Shunji Nomura[a] and Masayuki Imai[b]

[a]*Department of Polymer Science and Engineering, Kyoto Institute of Technology, Matsugasaki, Sakyo-ku, Kyoto 606, Japan*
[b]*Institute for Solid State Physics, The University of Tokyo, Roppongi, Bunkyo-ku, Tokyo, Japan*
(Received 3 June 1997; revised 12 August 1997; accepted 28 September 1997)

The crystallisation kinetics of the end-linked poly(tetrahydrofuran) (PTHF) network has been investigated in terms of small-angle neutron scattering (SANS). Fully deuterated PTHF (DPTHF, D) and hydrogenated PTHF (HPTHF, H), having degrees of polymerisation, $N_D = 166$ and $N_H = 142$, respectively, were blended before cross-linking. Two types of labeled network, one 5% and the other 50% hydrogenously labeled, were employed, where the major component was designed to be deuterated polymers in order to minimise the incoherent scattering. In the molten state ($T = 50$°C), the structure factors for both network and linear polymer blend are well described with the de Gennes' scattering intensity function for polymer blends. On the other hand, a significant domain scattering due to the presence of crystalline lamellar structure was observed in the solid state ($T = 20$°C for crystallisation time $= \infty$). During isothermal crystallisation, initiated by quenching the network film from 60 to 20°C, the radius of gyration of the labeled chain and the apparent interaction parameter, χ_{app}, increased slightly with time. This indicates that a crystallisation leads to miscibility reduction of the amorphous region. A scattering maximum, q_m, corresponding to the lamellar identity period, appeared and increased with time. The crystallisation for the network was found to be considerably slower than that of the corresponding linear polymer blends. These results were consistent with those obtained by small-angle X-ray scattering on the same system.

(Keywords: poly(tetrahydrofuran); crystallisation; small angle neutron scattering)

INTRODUCTION

Poly(tetrahydrofuran) (PTHF), equivalent to poly(tetramethylene glycol), is a crystalline polymer, the melting temperature of which lies around 40°C. Because crystallisation of PTHF takes place at ambient temperature (~20°C), the physical properties of PTHF change drastically around these temperatures[1]. PTHF is the so-called soft segment component of segmented polyurethane and polyurethane urea, which is physically cross-linked by hard segment domains (see, for example, Refs. [2,3]). Therefore, studies of the crystallisation kinetics of PTHF networks is of particular significance to understand the physical properties of these segmented block copolymers. In the first paper of this series[4], we reported the isothermal crystallisation kinetics of poly(tetrahydrofuran) (PTHF) networks using differential scanning calorimetry (d.s.c.) and optical microscopy. Due to the fatal structural constraint, i.e., the presence of cross-links, the crystallisation rate is greatly suppressed (with a factor of 1/10) compared with that of the corresponding linear polymers. In the second paper[5], small-angle X-ray scattering (SAXS) was employed to investigate the molecular weight dependence of the crystallisation kinetics. It was found that the crystallisation half time, $t_{1/2}$ is a decreasing function of the degree of polymerisation between cross-links, N, and there is a lower bound of N for isothermal crystallisation. Spherulite formation and a linear spherulite growth were clearly observed by polarised optical microscopy, indicating that the crystallisation is classified to heterogeneous nucleation with interfacial control. It was rather surprising that spherulites are formed in spite of a rather high density of cross-links (a cross-link is located at every 60 THF monomers along a chain). The following question was raised on the basis of the experimental findings described above: are the network chains contracted or stretched by crystallisation? Small-angle neutron scattering (SANS) is a means to answer this question.

SANS has been extensively employed for the studies of polymer crystallisation in the past two decades. In the case of melt crystallisation for polyethylene[6,7], polypropylene[7–9], and isotactic polystyrene[10], deuterated (and protonated polybutadiene)[11,12], it is known that the radius of gyration of the labeled chains, R_g, does not change by crystallisation. Ballard et al. reported that R_g scales with $M_w^{1\backslash 2}$, for quenched, annealed, and crystallised polypropylene, where M_w is the weight average molecular weight of the labeled polypropylene[8]. Sadler summarised recent SANS works with the emphasis of those on crystalline polymers[13]. Another important finding reported by them was that the scattered intensity, $I(q)$, decreases with q^{-2} for large q (q is the magnitude of the scattering vector), which indicates that the

* To whom correspondence should be addressed

molten chains are essentially described with Gaussian chains.

In the case of cross-linked polymers, effects of crystallisation on chain conformation has not been well elucidated. Thus, we conducted a time-resolved SANS study to solve this problem. First of all, we discuss the structure factor for end-linked PTHF networks in molten state. Then, we report the crystallisation kinetics of PTHF network investigated by time resolved SANS as well as by d.s.c.

THEORETICAL BACKGROUND

There are two major contributions to the SANS intensity function, $I(q)$, for a partially labeled network in a crystalline state; one is the scattering by deuterium (or hydrogen) labeling and the other is the domain scattering originating from a crystalline–amorphous two-phase structure. The former is obtained by measuring $I(q)$ in molten state. The latter may be extracted by subtracting the scattering from that of molten polymers. The difference in the scattering length between cross-links and the matrix can be another source of scattering, which will be discussed later.

The scattered intensity function, $I(q)$, for linear polymer blends in the molten state is calculated by de Gennes on the basis of the random phase approximation (RPA)[14,15], which is given by

$$\frac{v_0 k_N}{I(q)} = \frac{1}{\phi_D N_{D,w} g(q, N_{D,z})} + \frac{1}{\phi_H N_{H,w} g(q, N_{H,z})} - 2\chi \quad (1)$$

where v_0 is the reference volume, k_N is the neutron contrast factor, and χ is the Flory–Huggins interaction parameter between deuterated (D) and hydrogenated (H) polymers. $N_{i,w}$ and $N_{i,z}$ are the weight and z average degree of polymerisation, respectively. $g(q,N_{i,z})$ is the Debye function for a linear polymer having $N_{i,z}$ and is given by

$$g(q, N_{i,z}) \equiv \frac{2}{u_i^2}[\exp(-u_i) - 1 + u_i] \quad (2)$$

where u_i is the dimensionless parameter, given by

$$u_i \equiv \frac{N_{i,z} a^2 q^2}{6} = R_{g,i}^2 q^2 \quad (3)$$

and a and $R_{g,i}$ are the segment length and the radius of gyration of the i-component. The neutron contrast factor, k_N, is given by[15]

$$k_N = N_A \left(\frac{b_D}{v_D} - \frac{b_H}{v_H} \right)^2 \quad (4)$$

where N_A is the Avogadro's number, and b_i and v_i are the scattering length and the molar volume of the component i, respectively. The constant, $v_0 k_N$ is estimated to be 0.483 cm^{-1} for DPTHF and HPTHF, where we set $v_0 \equiv (v_D v_H)^{1/2}$.

EXPERIMENTAL SECTION

Samples

Two types of telechelic poly(tetrahydrofuran) (PTHF) prepolymers having allyl groups at the both ends were synthesised by living cationic polymerisation. One was the hydrogenated PTHF (HPTHF) and the other was fully deuterated PTHF (DPTHF). The details of sample preparation are described elsewhere[4,5]. In the case of DPTHF, deuterated THF monomer was purchased from Aldrich Chemical Co., the degree of deuteration of which was 99.5%. PTHF networks were prepared by cross-linking a mixture of HPTHF and DPTHF with a four-functional cross-linker, pentaerythritol tetrakis(3-mercaptopropionate). After preparation of networks, sol fraction was extracted by immersing the network in toluene repeatedly. The details of the cross-linking reactions and the characterisation method are given elsewhere. *Table 1* shows the sample code and characterisation of the prepolymers and networks. The number average degree of polymerisation, $N_{i,n}$ (i = D or H), was determined by vapor pressure osmometry (VPO, Knauer) by taking account of the molecular weight of the end groups. The weight and z average degree of polymerisation, $N_{i,w}$ and $N_{i,z}$, respectively, were estimated on the basis of gel permeation chromatography (g.p.c.) calibrated with standard polystyrenes.

D.s.c.

Samples of about 3 mg were crimped in an aluminum pan and heat treated at 60°C, which was higher than the melting temperature of PTHF, and then the samples were crystallised at a crystallisation temperature of $T_c = 20$°C for more than 1 day. After completion of crystallisation, d.s.c. was carried out with a DSC 3100 (MAC Science, Co. Ltd., heat flux type DSC). The heating rate was 5°C/min.

SANS

Small-angle neutron scattering (SANS) experiments were carried out at the research reactor SANS-U, Institute of Solid State Physics, The University of Tokyo, located at the

Table 1 Sample characterization

Sample code	Vol. fraction of DPTHF	Gel fraction[a]	VPO[b]		GPC[c]			
			$N_{D,n}$	$N_{H,n}$	$N_{D,w}$	$N_{H,w}$	$N_{D,z}$	$N_{H,z}$
Prepolymer								
P000	0	—		142	—	170	—	197
P100	100	—	166	—	189	—	212	—
Network								
N000	0	0.700	—	142	—	170	—	197
N050	50	0.814	166	142	189	170	212	197
N095	95	0.779	166	142	189	170	212	197
N100	100	0.711	166	—	189	—	212	—

[a]The gel fraction was estimated by measuring the weight after extraction of the sol component
[b]The number average degree of polymerization was estimated by vapor pressure osmometry, VPO
[c]The weight and z average degrees of polymerization were obtained by GPC

Japan Atomic Energy Research Institute, Tokai, Japan. Cold neutrons having a wavelength of $\lambda = 7.0$ Å were used as the incident beam. Each network sample was sealed in a brass cell having quartz windows, the typical optical path length of which was around 2 mm (e.g., 2.03 mm). The sample cell was mounted on a copper holder the temperature of which was regulated by a water circulating system (NESLab., Model RTE110). The temperature at the sample position was calibrated with a thermocouple sensor. Then the sample was irradiated by the neutron beam for 20 min and the scattered intensity was counted with an area detector. The observed scattered intensity was circularly averaged, corrected for cell scattering, transmission, the sample thickness, incoherent scattering, and fast neutrons, followed by rescaling to the absolute intensity with a secondary standard sample of a Lupolen[16].

RESULTS AND DISCUSSION

D.s.c.

Figure 1 shows the d.s.c. thermograms of networks (N000, N050, and N100 upper) and prepolymers (P000, P050, and P100; lower). Comparison of P and N series clearly indicates that both melting temperature, T_m, and enthalpy of fusion, ΔH, are suppressed by introduction of cross-links. A systematic lowering of the melting temperature, T_m, with composition is observed for the prepolymer from HPTHF to DPTHF. This is due to an isotope effect[17] in melting temperature as is well known for isotope polyethylenes[7]. For example, T_m of deuterated polyethylene (PE) is about 6°C lower than that of hydrogenous PE. However, in the case of networks, N050 has the lowest melting temperature. This may indicate that melting point depression, commonly observed in two-component systems, is another reason for the T_m variation with composition in addition to the isotope effect. Such a melting point depression is exclusively observed in the network. This is due to the presence of cross-links which suppresses crystallisation-induced phase separation between isotopes. It should be noted here that the temperatures chosen for the scattering experiments, 50°C (for molten samples) and 20°C (for crystallisation kinetics) were higher and lower enough than T_m, respectively.

Figure 2 shows (a) the enthalpy of fusion, ΔH, and (b) T_m for N000 and N100 crystallised for different crystallisation times t. It seems that crystallisation takes place within 1000 min, followed by gradual increase in T_m. Though the values of ΔH in the plateau region ($t > 1500$ min) are different between the isotopes, the reason is not clear at this stage. Similar crystallisation curves were obtained for N050 and N095.

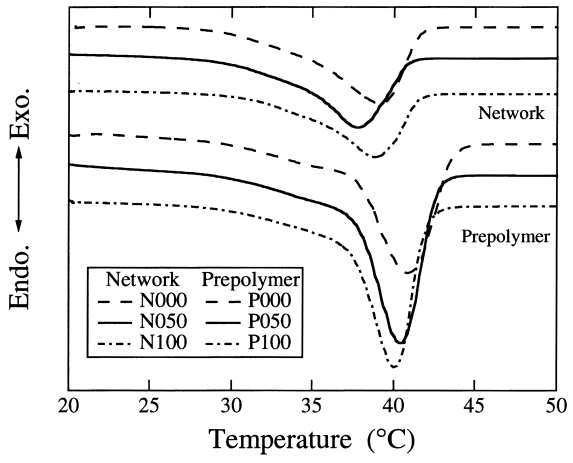

Figure 1 DSC thermograms of PTHF networks (N000, N050 and N100) and PTHF prepolymers (P000, P050, and P100)

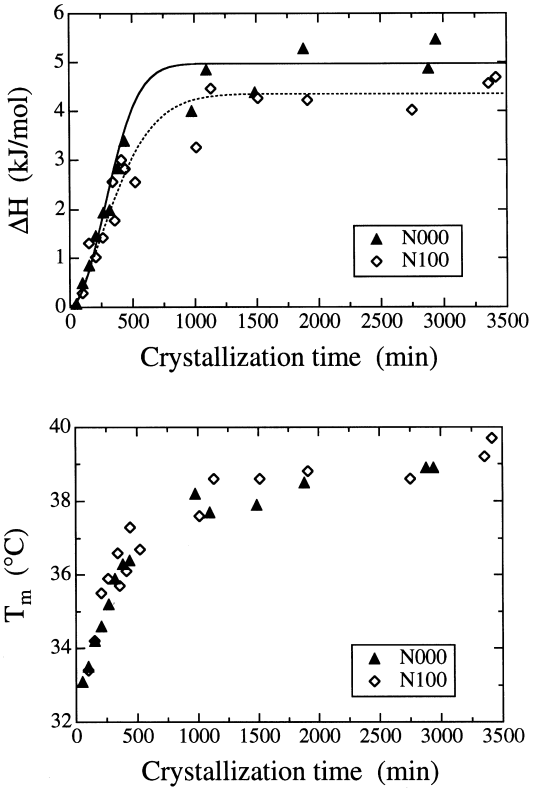

Figure 2 Crystallisation time dependence of the enthalpy of fusion, ΔH, and the melting temperature, T_m

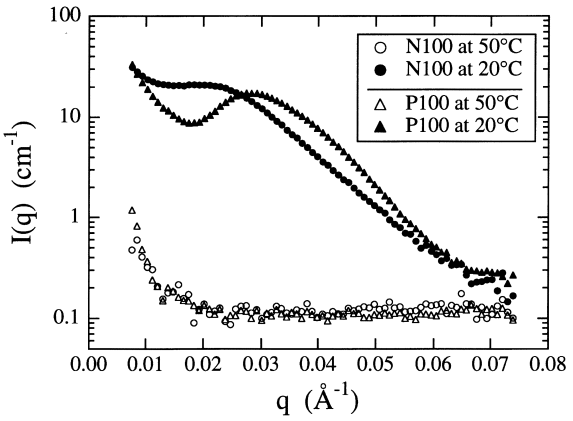

Figure 3 SANS intensity function, $I(q)$, for fully deuterated PTHF network and prepolymer observed at 50°C (molten state) and 20°C (crystalline state)

Scattering functions for homopolymer samples

Figure 3 shows the scattered intensity function, $I(q)$, for N100 and for P100 at 50°C (molten state) and 20°C (semicrystalline state). This figure discloses at least the following facts. (1) By comparing $I(q)$ values for the network and the prepolymer in the molten state, it is concluded that the contribution of the cross-links present in the network to SANS is negligible. (2) A considerable

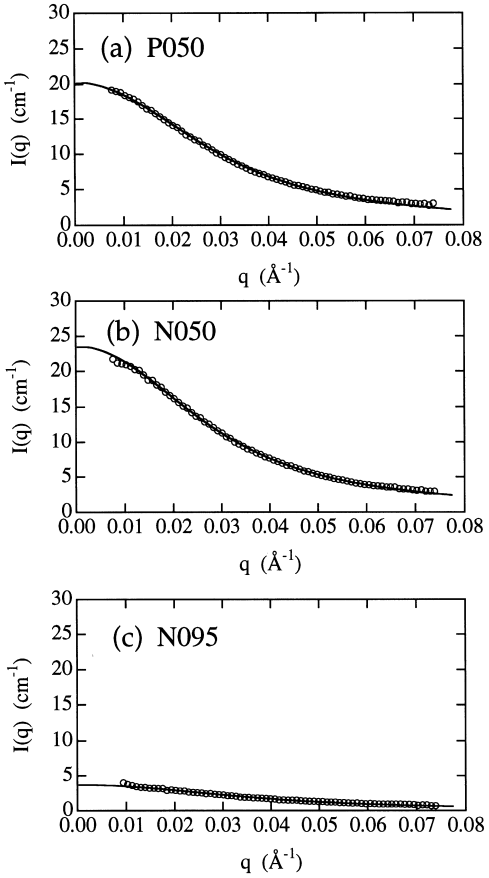

Figure 4 SANS intensity function, $I(q)$, for prepolymer blend (P050) and labeled networks (N050 and N095). The solid curves denote the theoretical functions for polymer blends

scattering is observed due to crystallisation. This corresponds to formation of crystalline lamellar domains (domain scattering). The domain identity period of the crystalline lamellar structure, L, is estimated to be 237 Å for N100 and 192 Å for P100. The difference in L values is ascribed to the difference in the rate of crystallisation between the network and prepolymer. The crystallisation rate of P100 is much faster than that of N100, resulting in a smaller L value[4].

Scattering functions for blends in molten state

Figure 4 shows $I(q)$ values for (a) prepolymer blend, P050, and polymer networks (b) N050 and (c) N095. Because the temperature was chosen to be 50°C, all of the samples were in molten state. The solid curves are the calculated scattered intensity functions with equation (1). The fitting range was 0.0112–0.0614 Å^{-1}. In the case of (a), N_D and $R_{g,D}$ were chosen to be the fitting parameters, and the following relations were used,

$$N_{H,w} = \left(\frac{N_{H,w}}{N_{D,w}}\right)_{GPC} N_{D,w} = 0.900 N_{D,w},$$

$$R^2_{g,H} = \left(\frac{N_{H,z}}{N_{D,z}}\right)_{GPC} R^2_{g,D} = 0.964 R^2_{g,D} \quad (5)$$

where $(N_{H,w}/N_{D,w})_{GPC}$ and $(N_{H,z}/N_{D,z})_{GPC}$ are the ratios of the degree of polymerisation and that of the radius of gyration estimated by GPC. Note that the radius of gyration obtained by scattering is the z average radius of gyration. Furthermore, the interaction parameter, χ, was set to be zero because χ for the isotope polymer mixtures is negligibly small. Thus, the number of floating parameters was restricted to 2, i.e., N_D and $R_{g,D}$. The results of the fitting are shown as the solid curve in *Figure 4a* and in *Table 2*. It may be criticised that the assumption $\chi = 0$ is too crude to evaluate $R_{g,D}$. However, the value of χ affects mainly N_D not $R_{g,D}$, and nonzero χ becomes significant when phase separation between amorphous isotope mixtures has to be considered. According to Bates and co-workers, such a phase separation in isotope mixtures is usually observed when the degree of polymerisation of the isotopes is larger than N_c (on the order of 10^3) (e.g., 2.3×10^3 for deuterious/hydrogenous polybutadiene, and 3.8×10^3 for deuterious/hydrogenous polystyrene)[18,19]. Since the degree of polymerisation in this system is one order lower than N_c, isotope-induced phase separation is not necessary to be considered. The curve fitting for the polymer networks was conducted by fixing $N_{D,w}$ and floating $R_{g,D}$ and χ. A curve fitting with three floating parameters ($N_{D,w}$, $R_{g,D}$, χ) was not successful because the structure factor was too sensitive to χ. Because the polymer networks, N050 and N095, consist of the same prepolymers as P050, the fixation of $N_{D,w}$ is reasonable. No adjustable parameter was used for the intensity scale. The results of curve fitting are shown in *Figure 4b* and *Figure 4c* and the fitting parameters are also listed in *Table 2*. The evaluated $R_{g,H}$ are 53.4 Å for P050 (the prepolymer blend)and 51.0 Å for N050 (the 50/50 network). These values are about 20% larger than the calculated value for the radius of gyration in the unperturbed state for HPTHF, $(R_{g,H})_0 = a < N_H > z^{1/2}$ of 41.8–43.5 Å, where a is the segment length of PTHF and is 7.3–7.6 Å[20]. Thus the observed $(R_{g,H})_0$ is slightly larger than the calculated one. This discrepancy may partially result from the fact that the degree of polymerisation of PTHF studied here is not large enough to apply the scattering function obtained by RPA. Such a positive deviation of R_g due to insufficient polymer chain length is also observed in polypropylene[8]. Note that the important finding here is not the value of R_g but the agreement in R_g values between the network and prepolymers. The introduction of the cross-links to the prepolymer blends does not seem to change the chain conformation as evidenced by the invariance of R_g values. The effect of cross-links appears as a slight increase in χ by 0.0017 (or a slight increase in the scattered intensity at $q = 0$ by about 3 cm^{-1}).

Isothermal crystallisation

The SANS study of crystallisation kinetics of PTHF

Table 2 RPA fitting results for the molecular parameters

Sample code	VPO		SANS fitting with RPA				
	$N_{D,w}$	$N_{H,w}$	$N_{D,w}$	$N_{H,w}$	$R_{g,D}$ (Å)	$R_{g,H}$ (Å)	χ
P050	189	170	178	160	55.4	53.4	(0)
N050	189	170	(178)	(160)	52.9	51.0	0.0017
N095	189	170	(178)	(160)	45.3	43.7	−0.0001

The numbers in the parentheses are fixed in the curve fitting procedure

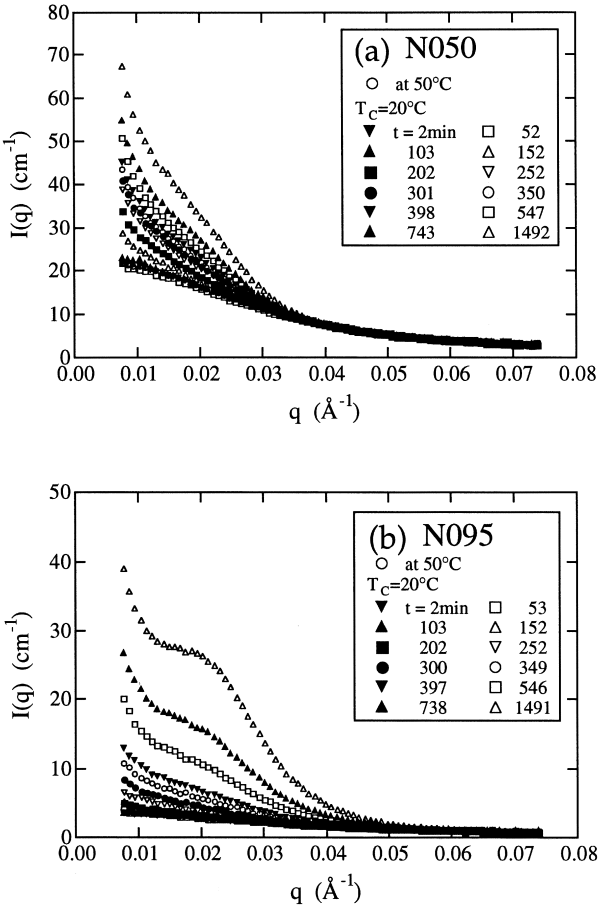

Figure 5 Time evolution of the SANS intensity functions, $I(q)$, for PTHF networks: (a) N050 and (b) N095

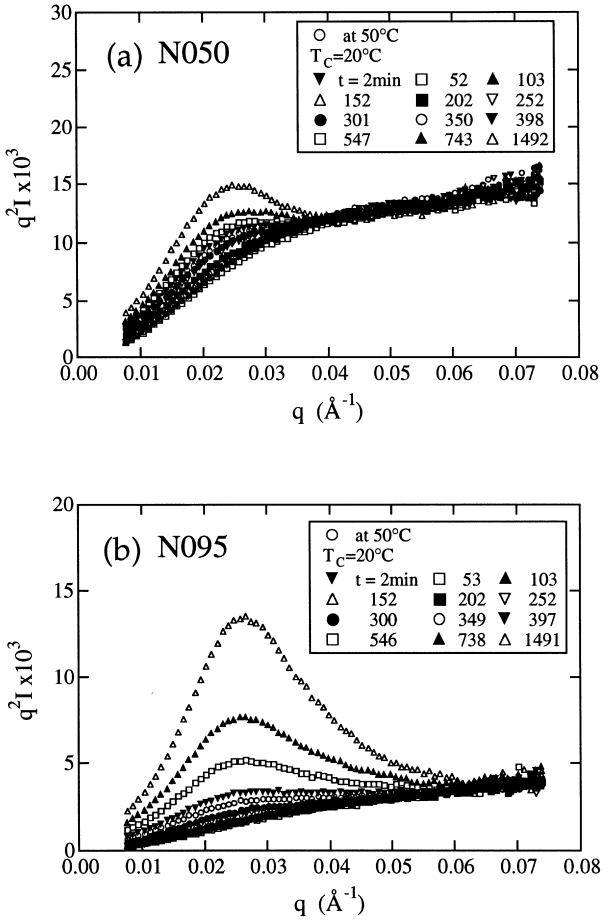

Figure 6 Lorentz-corrected SANS intensity functions, $q^2I(q)$, for PTHF networks: (a) N050 and (b) N095

networks was conducted by quenching sample films from 60°C (molten state) to the crystallisation temperature, T_c = 20°C. After quenching, SANS scattered intensity profiles were collected as a function of crystallisation time, t. *Figure 5* shows the time course of SANS intensity profiles for (a) N050 and for (b) N095. In both cases, it is clear that $I(q)$ increases with time. The increase in $I(q)$ with crystallisation time is explained with the following four contributions: (i) domain scattering due to formation of crystalline lamellar structure (around $q = q_m$); (ii) decrease in miscibility of the isotope blend (or segregation of deuterated and hydrogenated polymers); (iii) formation of higher order structures, e.g., spherulites; and (iv) void formation. Obviously, the domain scattering, (i), is the major contribution to the increase in $I(q)$. Therefore, we focus on the crystal formation here and discuss the rest of the contributions in the subsequent sections. It should be noted that (ii) may be important in the early stage of crystallisation, and that (iii) and (iv) become significant in the late stage. However, all of these contributions affect $I(q)$ at low angles since (ii) is related to the thermodynamics (i.e., the thermodynamic limit; $q = 0$) and (iii) and (iv) have a larger inhomogeneity than crystalline lamellae (i.e., $q \ll q_m$).

Figure 6 shows the Lorentz corrected scattered intensity plot, $q^2I(q)$ *versus* q, for (a) N050 and (b) N095 crystallised at 20°C. It is clear from this figure that crystalline structure formation leads to an excess scattering superimposed to the isotope scattering (blend scattering). Therefore it is convenient to introduce the excess scattering intensity function, $\Delta I(q)$, defined by

$$\Delta I(q) \equiv I(q) - I_{\text{molten}}(q) \tag{6}$$

where $I_{\text{molten}}(q)$ is the scattered intensity function at 50°C. *Figure 7* shows the Lorentz corrected scattered intensity for the excess scattering due to formation of crystals, $q^2\Delta I(q)$ *versus* q plot for (a) N050 and (b) N095. This clearly shows time evolution of the scattered intensity with a characteristic length scale, $L \equiv 2\pi/q_m$, where q_m is the magnitude of the scattering vector at the peak. Integration of $q^2\Delta I(q)$ of the peak area gives an index of the crystallinity. The integrated intensity, A, is defined by

$$A \equiv \int_{q_{\min}}^{q_{\max}} q^2 \Delta I(q) \mathrm{d}q \tag{7}$$

where $q_{\min}$ and $q_{\max}$ are the lower and upper bounds of the peak. We chose $q_{\min} = 0.0076$ Å^{-1} and $q_{\max} = 0.0480$ Å^{-1}, and obtained A as a function of the crystallisation time. The value of $q_{\min}$ was chosen as the lower limit of the SANS experiment in this work. This truncation may affect no more than 10% of the evaluation of A.

Figure 8 shows the time variation of A as well as L. Note that A is scaled to the absolute intensity, i.e., Å^{-2} cm^{-1}. Therefore, a direct comparison between A_{N050} and A_{N095} can be made. It is rather surprising that A_{N095} becomes much larger than A_{N050} at $t \geq 1500$ min. This indicates that (i) the degree of crystallisation of N095 is much higher than that of N050, or (ii) scattering due to spherulite formation or voids is more pronounced in N095 because of higher deuterium labeling than in N050.

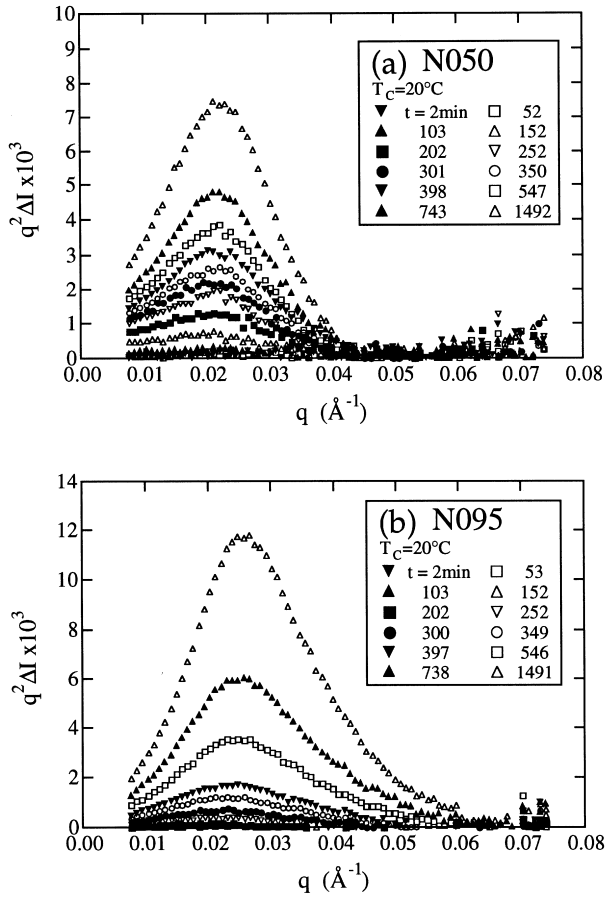

Figure 7 Excess scattered intensity, $q^2I(q)$ *versus* q plots for PTHF networks: (a) N050 and (b) N095

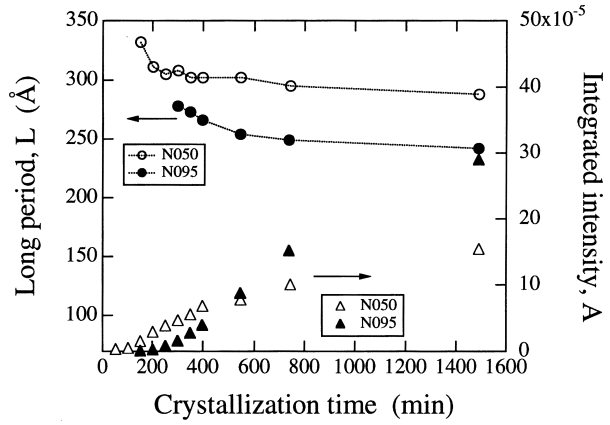

Figure 8 Crystallisation time dependence of the long period, L, and the integrated intensity, A, for PTHF networks

The lamellar identity period L becomes observable for t (>600 min) and is about 240 Å irrespective of the composition and of crystallisation time. In our previous paper, we observed $L \approx 200$ Å for U102 (equivalent to N000) by small-angle X-ray scattering[4]. The discrepancy between the two L values is due to the difference in the crystallisation temperature; 20°C (this work) and 15°C (the previous work). It is reasonable that a higher crystallisation temperature leads to a larger value of L.

Chain scattering during isothermal crystallisation

Figure 9 shows Guinier plots of the SANS intensity

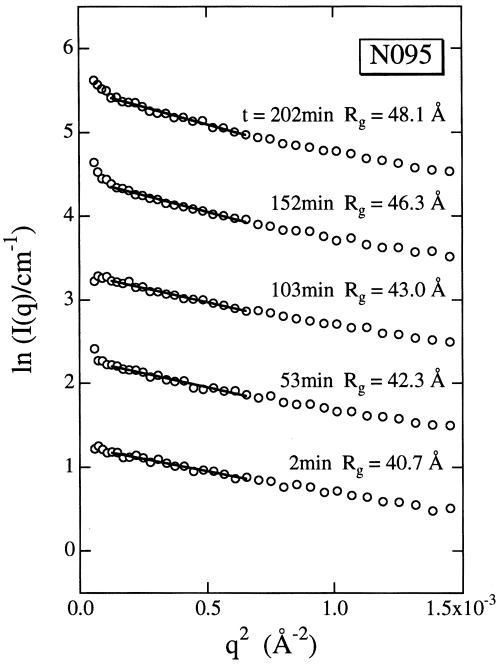

Figure 9 Guinier plots for the scattered intensity for N095 in the early stage of isothermal crystallisation at 20°C

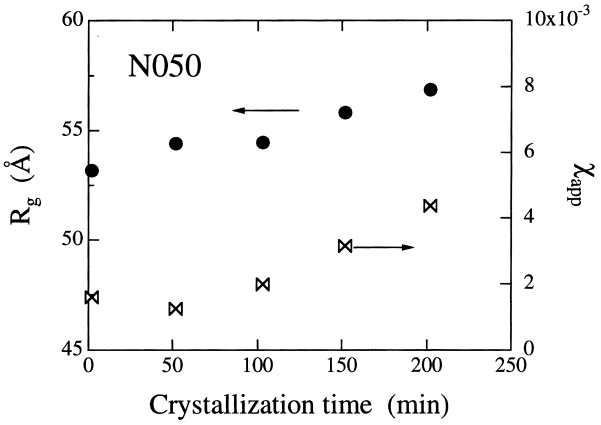

Figure 10 Crystallisation time dependence of the radius of gyration, R_g, and the apparent interaction parameter, χ, for N050 in the early stage of isothermal crystallisation at 20°C

function for N095 during crystallisation. The scattered intensity function for the labeled chains is given by,

$$\ln I(q) = \text{const.} - \frac{R_g^2}{3} q^2 \qquad (8)$$

At $t = 0$, R_g is estimated to be 40.7 Å. With increasing t ($\leq$ 202 min), R_g slightly increases as shown in the figure. For larger t values the Guinier analysis was impossible due to strong scattering at the low q region. A curve fitting with equation (1) was also applied to estimate R_g in the same time range, and $R_{g,H}$ was estimated to be 43.7 Å (*Table 2*), which agrees well to that obtained by the Guinier analysis (40.7 Å).

Since equation (1) is not applicable to polymer blends in crystalline state, we conducted curve fitting for N050 only at the beginning of isothermal crystallisation, where we assume that crystalline embryos do not seriously change the scattering function for their molten state. *Figure 10* shows the crystallisation time dependence of R_g and the

apparent interaction parameter, χ_{app}, for N050. We use here χ_{app} instead of χ because the evaluated interaction parameter from $I(q = 0)$ with equation (1) is influenced by the low-angle scattering and crystal domain scattering. Similar to the case of N095 (*Figure 9*), R_g slightly increases with t. The increase in the scattered intensity results in an increase of χ_{app}. This increases noticeably with t, which is partially due to a lowering of the miscibility between the isotope chains. Note that we restricted the crystallisation time window to less than 250 min so as to avoid the effect of artifact, i.e., the very beginning part of the crystallisation process (the degree of crystallisation being less than 3% on the basis of d.s.c.).

On the basis of the SANS results shown above, we conclude that polymer chains are slightly stretched on crystallisation. This is partly explained as follows: crystal formation in the network is dominated by random reentry rather than adjacent reentry since chain contraction is expected for adjacent reentry[13]. In addition, increasing topological constraint, i.e., physical cross-links due to crystalline formation in addition to the chemical cross-links, leads to an increase of the radius of gyration.

Generation of spatial inhomogeneity during isothermal crystallisation

In order to interpret the SANS results shown above, the contribution of the low-angle scattering has to be seriously taken into account. Problems in the studies of crystallisation with SANS have been extensively discussed by Schelten et al.[6]. These are (1) segregation of the labeled chains during crystallisation and (2) void formation. Note that it is not necessary to consider phase separation due to isotopes here because the degree of polymerisation of the polymers studied is much lower than N_c, as discussed in *Figure 4*. The former is due to the difference in the melting temperatures, which is not serious for isotope networks because segregation is inherently impossible due to the chemical constraints. In order to suppress void formation, Schelten et al. used hydrogenous PE for matrix and deuterated PE as a labeled species[6]. This greatly reduces the void scattering since the scattering length of hydrogenous PE ($-CH_2-$) is nearly equal to zero because of cancellation of the scattering length by the combination of CH_2, i.e., ^{12}C ($b = 6.657 \times 10^{-13}$ cm), and ^{1}H ($b = -3.739 \times 10^{-13}$ cm). In this work, however, we designed the labeled network with 50 and 95% deuterium-substituted PTHF. The reason was to reduce strong incoherent scattering of ^{1}H. In the case of the time-resolved SANS experiment, it is essential to increase the signal-to-noise ratio. Since the incoherent scattering simply raises the noise scattering, it was important to design a mixture having a large concentration of deuterated component.

Void formation has been thought to be one of the reasons for the strong low-angle scattering in crystalline polymers. This is true for solution-grown polymer crystals, since the presence of voids can be verified by microscopy or scattering experiment on the crystal, the voids of which are filled with liquid. However, it is doubtful, for melt-grown polymer crystals, to ascribe the increase in the scattered intensity to void formation. No vivid proof of voids has been reported so far. It is noteworthy that a noticeable increase in scattering is commonly observed in glassy polymer by cooling from its melt where no void formation takes place (for example Ref. [21]). The intensity increase has been interpreted by creation of a long-range inhomogeneity. A similar phenomenon may occur in crystalline polymer during isothermal crystallisation. Therefore, we do not believe that the scattering is due to void formation. On the other hand, we know that an isothermal crystallisation of PTHF networks gives rise to spherulite formation[4,5]. Since the size of these spherulites are on the order of a few tens of micrometers, strong concentration fluctuations, the wavelength of which is from manometers to submillimeters, are created by isothermal crystallisation. The formation of these spatial inhomogeneities must be the major reason for the strong low-angle scattering. Because of these reasons, the analysis of the R_g during isothermal crystallisation was limited to the very beginning of crystallisation.

CONCLUDING REMARKS

Small-angle neutron scattering experiments were conducted on end-linked poly(tetrahydrofuran) (PTHF) networks consisting of deuterated and hydrogenated PTHF chains. In the molten state, the scattered intensity function, $I(q)$, for the network is nearly identical to that for the prepolymer blends. Both structure factors are well described by the de Gennes scattering function for linear polymer blends. This clearly indicates that the structure factor is not noticeably modulated by introduction of cross-links. The estimated R_g and the degree of polymerisation were somewhat larger than calculated ones, but those values are within an experimental error. Isothermal crystallisation at 20°C led to a slight increase in R_g and the apparent interaction parameter, χ_{app}, at the beginning, followed by an appearance of a scattering peak at $q_m \approx 0.026$ Å^{-1}. The estimation of R_g was thus limited only at the beginning of crystallisation. The lamellar spacing evaluated from q_m was about 240 Å and was invariant with crystallisation time. The time variation of the integrated intensity of the peak estimated from the plot of $q^2I(q)$ *versus* q is similar to the time variation of the enthalpy of fusion of the crystallised network.

ACKNOWLEDGEMENTS

This work is partially supported by the Grant-in-Aid, Ministry of Education,Science and Culture, Japan (Grant-in-Aid, Nos. 07241242, 08231245, and 09450362 to MS). This work was performed with the approval of the Solid State Physics Laboratory, The University of Tokyo (Proposal No.5744) at Japan Atomic Energy Research Institute, Tokai, Japan.

REFERENCES

1. Dreyfuss, P., *Poly(tetrahydrofuran)*. Gordon and Breach Sci. Pub., NY, 1982.
2. Ratner, B. D., in: *Comprehensive Polymer Science*. ed. S. L. Aggarwal. Pergamon, New York, 1988.
3. Petrovic, Z.S. and Ferguson, J., *Prog. Polym. Sci.*, 1991, **16**, 695.
4. Shibayama, M., Takahashi, H. and Nomura, S., *Polymer*, 1994, **35**, 2944.
5. Takahashi, H., Shibayama, M. and Nomura, S., *Macromolecules*, 1995, **28**, 5547.
6. Schelten, J., Wignall, G.D. and Ballard, D.G.H., *Polymer*, 1974, **15**, 682.
7. Schelten, J., Ballard, D.G.H., Wignall, G.D., Longman, G.W. and Schmatz, W., *Polymer*, 1976, **17**, 751.
8. Schelten, J., Wignall, G.D., Ballard, D.G.H. and Longman, G.W., *Polymer*, 1977, **18**, 1111.
9. Ballard, D.G.H., Cheshire, P., Longman, G.W. and Schelten, I., *Polymer*, 1978, **19**, 379.

10. Guenet, J.M., *Polymer*, 1980, **21**, 1385.
11. Crist, B., Graessley, W.W. and Wignall, G.D., *Polymer*, 1982, **23**, 1561.
12. Tanzer, J.D., Bartels, C.R., Crist, B. and Graessley, W.W., *Macromolecules*, 1984, **17**, 2708.
13. Sadler, D. M., in: *Comprehensive Polymer Science*, Vol. 2. ed. C. Booth and C. Price. Pergamon Press, Oxford, UK, 1989.
14. de Gennes, P.-G., *Scaling Concepts in Polymer Physics*. Cornell University Press, Ithaca, NY, 1979.
15. Shibayama, M., Yang, H., Stein, R.S. and Han, C.C., *Macromolecules*, 1985, **18**, 2179.
16. Schwahn, D., Takeno, H., Willner, L., Hasegawa, H., Jinnai, H., Hashimoto, T. and Imai, M., *Phys. Rev. Lett.*, 1994, **73**, 3427.
17. Buckingham, A.D. and Hentschel, H.G.E., *J. Polym. Sci., Polym. Phys. Ed.*, 1980, **18**, 853.
18. Bates, F.S., Wignall, G.D. and Koehler, W.C., *Phys. Rev. Lett.*, 1985, **55**, 2425.
19. Bates, F.S. and Wignall, G.D., *Macromolecules*, 1986, **23**, 932.
20. Brandrup, J., Immergut, E. H. (eds.), *Polymer Handbook*, 3rd edn. Wiley, NY, 1989.
21. Weber, H., Paul, W., Kob, W. and Binde, K., *Phys. Rev. Lett.*, 1997, **78**, 2136.